Electronic Supplementary Material (ESI) for Journal of Materials Chemistry C.

Supplementary Information

Unveiling the significance of adduct formation between thiocarbonyl Lewis donors and diiodine for the structural organization of rhodanine-based small molecule semiconductors

Anna Laura Sanna,[a] Simone Acca,[a] Enrico Podda,[b] Antonello Mascia,[c] Anna Pintus,[a] M. Carla Aragoni,[a] Vito Lippolis,[a] Carlo Ricci,[d] Piero Cosseddu,[c] Massimiliano Arca,[a*] and Giuseppe Sforazzini [a*]

[a] *Department of Chemical and Geological Science, University of Cagliari, S.p. no. 8 km 0.700, 09042 Monserrato, Cagliari, Italy*

[b] *Centro Servizi di Ateneo per la Ricerca (CeSAR), University of Cagliari, S.p. no. 8 km 0.700, 09042 Monserrato, Cagliari, Italy*

[c] *Department of Electrical and Electronic Engineering, University of Cagliari, Piazza d'Armi, 09123 Cagliari, Italy*

[d] *Department of Physics, University of Cagliari, S.p. no. 8 Km 0.700, 09042 Monserrato, Cagliari, Italy*

Content

1. Experimental section

Materials and Methods

All solvents and reagents were used as commercially supplied, without further purification. All the solvents 1,2-dichloroethane, dichlorometane, ethanol, ethyl acetate, petroleum ether 40-60 °C, acetonitrile and toluene were purchased from Carlo Erba Reagents. $POCl_3$ (99%) was purchased from Sigma Aldrich; dimethylformamide (DMF, 99.0%), 2,2'-bithiophene (99%), sodium acetate (99.0%); piperidine (99+%) and sodium sulfate (99+%, anhydrous) were purchased from Carlo Erba Reagents and 3-ethyl-2-thioxo-1,3-thiazolidin-4-one (98.0%) and I_2, were purchased from TCI.

Organic reactions were monitored by thin-layer chromatography (TLC) performed on alugram precoated silica sheets, 0.2 mm plates (MN), and compounds were visualized under UV light (254 nm or 365 nm), depending on the substrate. Column chromatography was performed on silica gel 60A (particle size 40 – 63 µm, Carlo Erba) under positive air pressure. ^{1}H and ^{13}C liquid NMR spectra were recorded on a Bruker Advance III HD 600 MHz NMR spectrometer at 298 K. Deuterated chloroform was used for the NMR sample preparation and was purchased from Carlo Erba Reagents. Chemical shifts (δH and δC) are expressed in parts per million (ppm) relative to the residual solvent peak and, for proton NMR, shown as follows: chemical shift, multiplicity (s = singlet, d = doublet, t = triplet, q = quartet, m = multiplet) and integration. Mass analyses were performed on an Exploris 240 LC/GC-Orbitrap FTMS mass spectrometer. IR measurements were recorded using a JASCO FTIR-4XLE spectrometer (ATR mode). Melting points were determined in capillaries on a FALC apparatus mod. C (up to 290 °C) melting point apparatus. Elemental analyses were performed with a CHN PE 2400 series II elemental analyzer (T = 925 °C).

X-ray Diffraction Measurements

X-ray single-crystal diffraction data for **BTR** and **BTR•I_2** were collected at 100 K on a Bruker D8 Venture diffractometer equipped with a PHOTON II detector. The structures were solved with the ShelXT[3] solution program using dual methods, and the models were refined with ShelXL 2018/3[4] using full-matrix least-squares minimization on F^2. Olex2 1.5[5] was used as the graphical interface. Hydrogen atom positions were calculated geometrically and refined using the riding model. CCDC 2341835 and 2341836 contain the supplementary crystallographic data for this paper. These data can be obtained free of charge from the Cambridge Crystallographic Data Centre.

Raman Spectroscopy

FT-Raman spectra were recorded at room temperature in the 80–2600 cm^{-1} range on SOL Instrument MS750 series spectrometer fitted with a laser CoherentOndaX LM series and operating with an excitation frequency of 785 nm.

2. Synthesis and Characterization

2.1. Synthesis of BTA and BTR

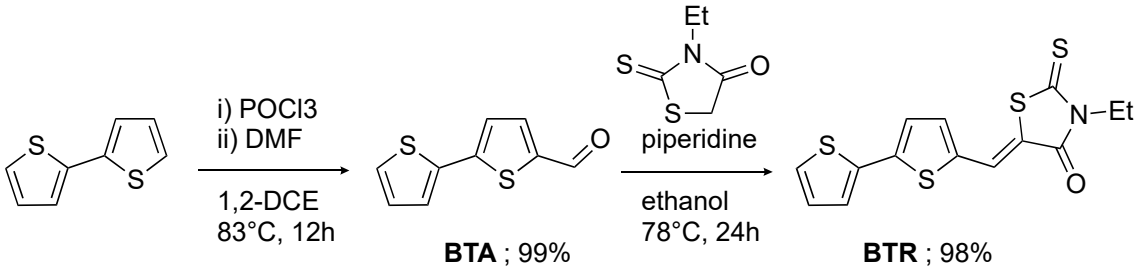

Scheme S1: Synthetic scheme for the preparation of **BTR**.

2,2'-bithiophene-5-carbaldehyde (**BTA**)**.** The title compound was synthesized adapting a literature procedure.[1] The Vilsmeier reagent was prepared by stirring $POCl_3$ (0.56 mL, 6.02 mmol) and DMF (0.46 mL, 6.0 mmol) for 10 minutes and then added to an ice-cold solution of 2,2'-bithiophene (0.500 g, 3.01 mmol) in 1,2-dichloroethane (4 mL). The reaction mixture was heated to reflux for 24 h, hydrolyzed with saturated aqueous sodium acetate solution for 6 h, and extracted three times with dichloromethane (100 mL). The organic layers were collected together, then dried over anhydrous sodium sulfate and filtered. The solvent was removed under vacuum to obtain the pure product as a yellow powder (0.580 g, 99 %). The product was used in the next step without further purification. ^{1}H NMR ($CDCl_3$) δ (ppm): 9.87 (s, 1 H), 7.67 (d, *J* = 3.9 Hz, 1 H), 7.36 (d, *J* = 4.4 Hz, 2 H), 7.25 (d, *J* = 3.9 Hz, 1 H), 7.08 (t, *J* = 4.4 Hz, 1 H). ^{13}C NMR (151 MHz, $CDCl_3$) δ (ppm) 182.6, 147.3, 141.8, 137.4, 136.2, 128.5, 127.2, 126.3, 124.4. The characterization of this compound is consistent with that found in the literature.[2]

(Z)-5-([2,2'-bithiophen]-5-ylmethylene)-3-ethyl-4-thioxothiazolidin-2-one (**BTR**) Piperidine (0.053 mL, 0.52 mmol) was added to a solution of compound **BTA** (0.200 g, 1.03 mmol) and 3-ethyl-2-thioxo-1,3-thiazolidin-4-one (0.182 g, 2.00 mmol) in 20 mL of ethanol under Argon atmosphere. The reaction mixture was stirred at reflux for 24 h, then quenched with water and extracted three times with ethyl acetate (100 mL). The organic layers were combined, dried with anhydrous sodium sulfate and filtered. The solvent was removed under reduced pressure and the crude product was purified by silica chromatography (DCM/Petroleum Ether = 6:4) to give a bright orange powder (0.346 g, 98 %). ^{1}H NMR (600 MHz, $CDCl_3$) δ (ppm): 7.83 (s, 1H), 7.34 (d, *J* = 4.9 Hz, 1H), 7.33 (d, *J* = 4.9 Hz, 2H), 7.24 (d, *J* = 3.9 Hz, 1H), 7.08 (t, *J* = 3.9 Hz, 1H), 4.18 (q, J = 7.1 Hz, 2H), 1.29 (t, J = 7.1 Hz, 3H). ^{13}C NMR (151 MHz, $CDCl_3$) δ (ppm): 192.1, 167.5, 145.6, 136.7, 136.3, 135.3, 128.5, 126.7, 125.6, 125.21, 125.17, 120.8, 40.1, 12.4. HRMS (ESI, positive mode) *m/z* calculated for $C_{14}H_{12}NOS_4$ $[M + H]^+$: 337.9802; found: 337.9788. M.p. 164 °C. Elemental analysis (Calcd. for $C_{14}H_{11}NOS_4$) C 45.94 (49.82), H 1.09 (3.28), N 3.99 (4.15). IR (2000–400 cm^{-1}): 507, 792, 1122, 1224, 1315, 1581, 1697, 1976, 2032, 2360. Raman (2600–80 cm^{-1}; most intense peak taken equal to 10.0): 428 (2.1), 864 (2.1), 1437 (10.0), 1531 (3.0), 1577 (4.7).

2.2. NMR spectra - Compound BTR (^{1}H and ^{13}C)

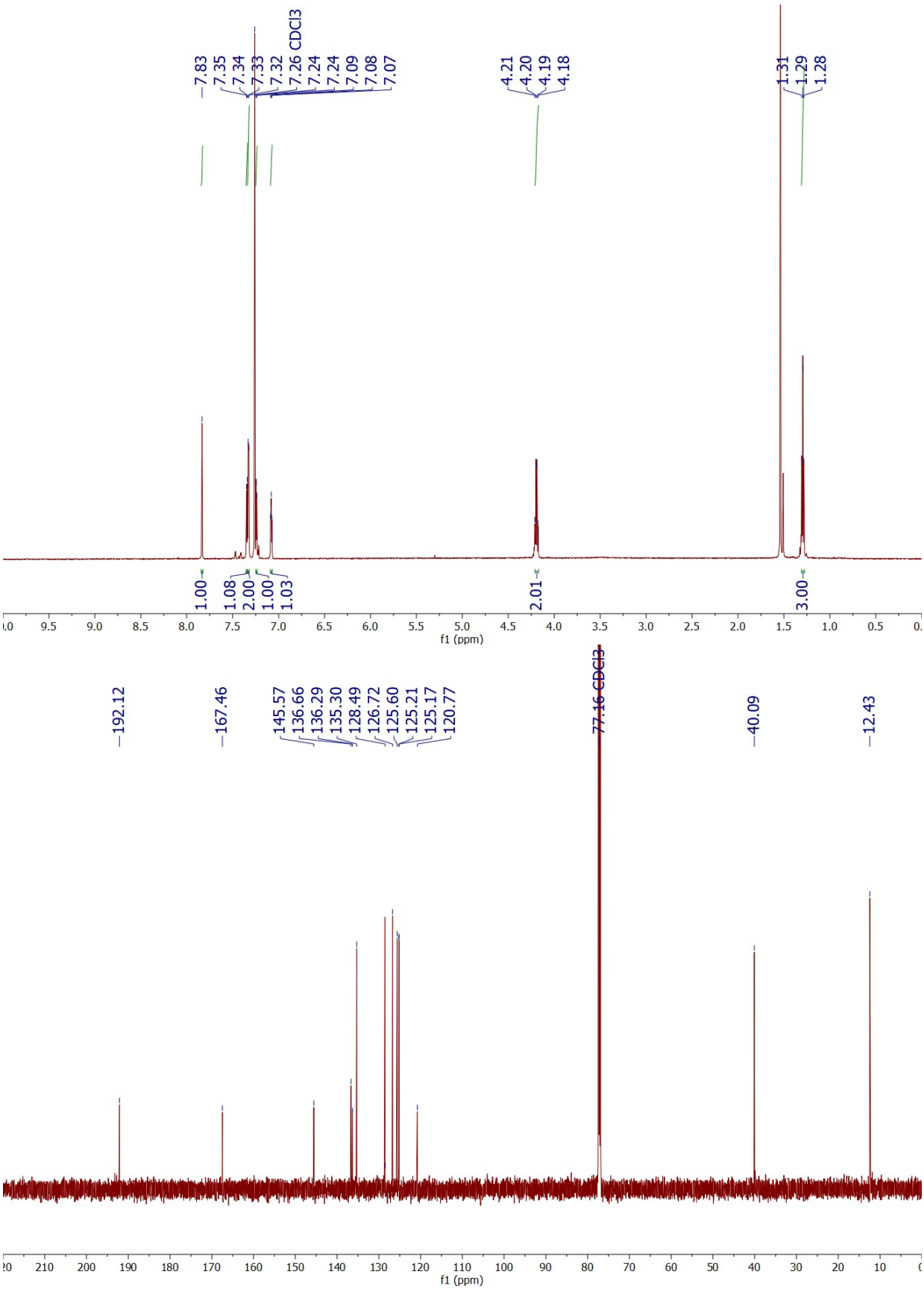

3. Crystals Preparation and Characterization

The crystals adduct were obtained using two methods.

Method A: Sublimation of iodine vapour into a hexane solution of **BTR**.

Method B: Dropwise addition of a solution of diiodine in hexane to a solution of the **BTR** in the same solvent. **BTR** and I_2 solutions were combined in 5:1 molar ratios [I_2]:[**BTR**]. Subsequently, crystals were isolated after 4–5 days at room temperature.

Compound **BTR·I_2** was obtained by both **Method A** and **Method B**. M.p. 154 °C. Elemental analysis ($C_{14}H_{11}NOS_4I_2$) C 34.46 (28.43), H 3.31 (1.87), N 2.71 (2.36). IR (2000–400 cm^{-1}): 509, 796, 1116, 1229, 1318, 1507, 1698, 1867, 2348.

Crystals of **BTR** were obtained through slow evaporation from ethanol. Characterization was reported in Section 2.1.

3.1. Crystal Data Analysis

Table S1 Crystal data and structure refinement parameters for compounds **BRT** and **BRT·I_2**.

Compound	**BRT**	**BRT·I_2**
Empirical formula	$C_{14}H_{11}NOS_4$	$C_{14}H_{11}I_2NOS_4$
Formula weight/g mol^{-1}	337.48	591.28
T/K	100(2)	100(2)
Crystal system	monoclinic	triclinic
Space group	$P2_1/c$	$P\bar{1}$
a/Å	6.1277(5)	8.9908(9)
b/Å	29.436(2)	10.5236(10)
c/Å	7.9018(7)	11.0589(11)
α/°	90	108.366(3)
β/°	93.267(3)	106.358(4)
γ/°	90	98.198(4)
V/Å^3	1423.0(2)	921.59(16)
Z	4	2
ρ_{calc}/ g cm^{-3}	1.575	2.131
μ/mm^{-1}	0.660	3.865
Crystal size/mm^3	0.12 × 0.11 × 0.07	0.21 × 0.09 × 0.03
Radiation	Mo*Kα* (λ = 0.71073)	Mo*K*α (λ = 0.71073)
2θ range for data collection/°	5.346 to 54.958	4.882 to 54.968
Reflections collected	26154	27834
Independent reflections	3266 [R_{int} = 0.0689, R_{sigma} = 0.0392]	4230 [R_{int} = 0.0303, R_{sigma} = 0.0182]
Data/restraints/parameters	3266/0/196	4230/0/216
GooF on F^2	1.056	1.051
Final R indexes [I ≥ 2σ (I)]	R_1 = 0.0350, wR_2 = 0.0669	R_1 = 0.0145, wR_2 = 0.0351
Final R indexes [all data]	R_1 = 0.0536, wR_2 = 0.0751	R_1 = 0.0162, wR_2 = 0.0360
Largest diff. peak/hole / e Å^{-3}	0.31/−0.27	0.48/−0.31

Table S2 Bond lengths (Å) for compound **BRT**.

S5–C11	1.656(7)	C15–C11	1.410(11)
S5–C13	1.567(6)	C15–C14	1.577(15)
S3–C7	1.734(2)	C7–C8	1.372(3)
S3–C10	1.726(2)	C7–C6	1.426(3)
S2–C3	1.748(2)	C2–C3	1.470(3)
S2–C1	1.746(2)	C3–C6	1.349(3)
S1–C1	1.632(2)	C9–C8	1.398(3)
S4–C11	1.695(3)	C9–C10	1.373(3)
S4–C14	1.632(3)	C11–C12	1.399(12)
O1–C2	1.210(2)	C11–C10	1.442(3)
N1–C2	1.398(2)	C4–C5	1.510(3)
N1–C1	1.365(3)	C14–C13	1.347(3)
N1–C4	1.464(2)	C13–C12	1.469(14)

Table S3 Bond angles (°) for compound **BRT**.

C13–S5–C11	94.6(4)	N1–C1–S2	110.67(14)
C10–S3–C7	92.24(10)	N1–C1–S1	127.18(16)
C1–S2–C3	92.40(10)	C15–C11–S5	112.0(6)
C14–S4–C11	93.47(14)	C15–C11–C10	125.7(6)
C2–N1–C4	120.57(16)	C12–C11–S4	110.2(6)
C1–N1–C2	116.90(17)	C12–C11–C10	128.0(6)
C1–N1–C4	122.52(16)	C10–C11–S5	122.3(2)
C11–C15–C14	108.3(8)	C10–C11–S4	121.76(16)
C8–C7–S3	110.12(15)	C7–C8–C9	113.73(18)
C8–C7–C6	127.10(19)	N1–C4–C5	111.68(17)
C6–C7–S3	122.78(15)	C13–C14–S4	115.73(18)
O1–C2–N1	123.10(19)	C13–C14–C15	105.0(4)
O1–C2–C3	127.00(18)	C14–C13–S5	119.9(3)
N1–C2–C3	109.90(17)	C14–C13–C12	109.2(5)
C2–C3–S2	110.09(14)	C11–C12–C13	111.3(9)
C6–C3–S2	128.15(16)	C3–C6–C7	128.70(19)
C6–C3–C2	121.76(18)	C9–C10–S3	110.59(15)
C10–C9–C8	113.31(19)	C9–C10–C11	129.51(19)
S1–C1–S2	122.15(12)	C11–C10–S3	119.85(15)

Table S4 Bond lengths (Å) for compound **BRT•I_2**.

I1–I2	2.8057(3)	C3–C6	1.354(2)
I1–S1	2.7576(5)	C4–C5	1.521(3)
S2–C1	1.7305(17)	C6–C7	1.424(2)
S2–C3	1.7510(17)	C10–C11	1.447(2)
S1–C1	1.6657(17)	C10–C9	1.374(2)
S3–C10	1.7270(17)	C7–C8	1.382(2)
S3–C7	1.7333(17)	C11–S4A	1.7215(19)
S4B–C11	1.675(12)	C11–C12A	1.381(9)
S4B–C13	1.542(13)	C11–C12B	1.43(2)
O1–C2	1.210(2)	C13–C14	1.361(3)
N1–C1	1.349(2)	C13–C12A	1.402(11)
N1–C2	1.410(2)	C14–S4A	1.688(2)
N1–C4	1.471(2)	C14–C12B	1.54(3)
C3–C2	1.463(2)	C8–C9	1.400(3)

Table S5 Bond angles (°) for compound **BRT•I_2**.

S1–I1–I2	174.695(10)	C9–C10–S3	110.86(13)
C1–S2–C3	91.66(8)	C9–C10–C11	129.06(16)
C1–S1–I1	104.27(6)	C6–C7–S3	124.14(13)
C10–S3–C7	92.13(8)	C8–C7–S3	110.32(13)
C13–S4B–C11	93.1(5)	C8–C7–C6	125.53(16)
C1–N1–C2	115.98(14)	C10–C11–S4B	122.8(4)
C1–N1–C4	123.31(14)	C10–C11–S4A	119.50(13)
C2–N1–C4	120.70(14)	C12A–C11–C10	130.9(4)
S1–C1–S2	123.68(10)	C12A–C11–S4A	109.6(4)
N1–C1–S2	112.32(12)	C12B–C11–S4B	109.9(12)
N1–C1–S1	124.00(13)	C12B–C11–C10	127.3(10)
C2–C3–S2	110.44(12)	C14–C13–S4B	123.9(4)
C6–C3–S2	127.85(14)	C14–C13–C12A	110.8(3)
C6–C3–C2	121.70(16)	C13–C14–S4A	113.48(14)
O1–C2–N1	122.45(16)	C13–C14–C12B	101.8(7)
O1–C2–C3	127.97(16)	C7–C8–C9	113.36(16)
N1–C2–C3	109.58(14)	C10–C9–C8	113.34(16)
N1–C4–C5	111.59(15)	C14–S4A–C11	91.91(9)
C3–C6–C7	129.27(16)	C11–C12A–C13	114.2(5)
C11–C10–S3	120.08(13)	C11–C12B–C14	111.3(14)

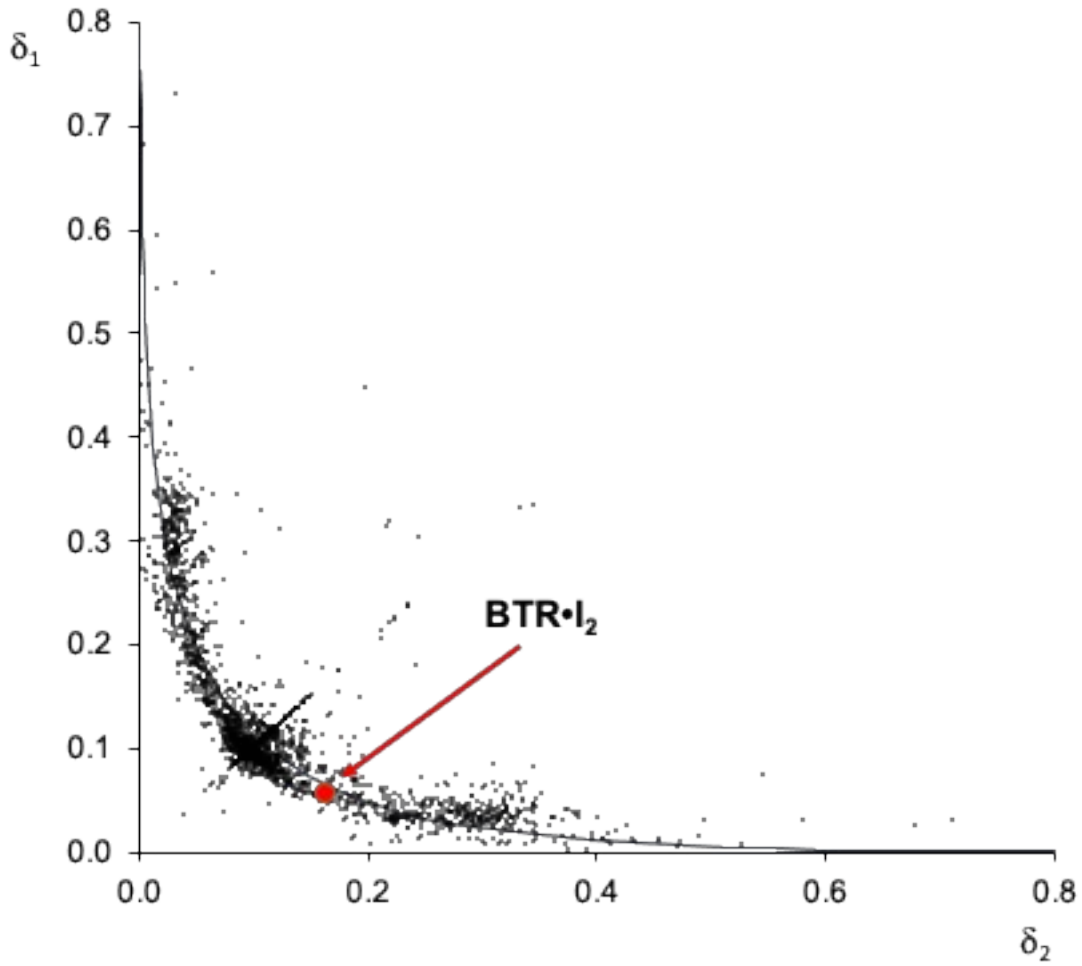

Figure S1. Structural data of linear A–B–C fragments deposited at the CSD reported as scatter plot of δ_1 vs. δ_2, where δ_1 = δ(A–B) and δ_2 = δ(B–C). Structural data were taken from ref. 5. The red dot represents the data for the S···I–I fragment in the structure of **BTR•I_2**. The solid curve represents the least-squares fit of all data according to the following equation: $\delta_1 = -k \cdot \ln[1-e(-\delta_2/k)]$: Fitted parameter: k = 0.153, RMSD = 0.043, normalized RMSD = 0.057.

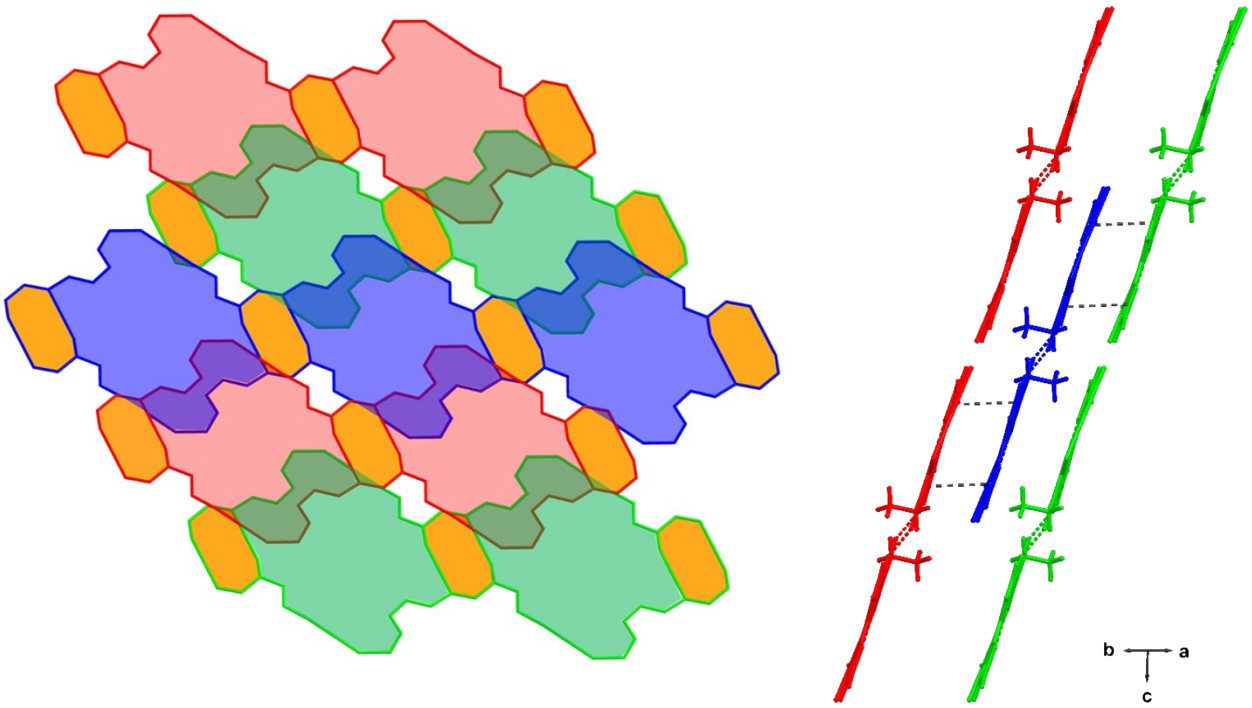

(a) (b)

Figure S2. Partial views a) along the [100] direction and b) along the [110] direction showing the relative orientations of adjacent ribbons in the crystal packing of **BTR•I_2**.

4. Raman Spectroscopy

Measurements were taken on at least three sample points in order to ensure uniformity of the experimental data. No decomposition of sample occurred during any of the experiments. Raman spectroscopy was used to characterize the diiodine adduct of **BTR** (**BTR·I_2**) as shown in Figure S3. The iodine stretching peak in the adduct **BTR•I_2** is shown at 150 cm^{-1} (Figure S3).

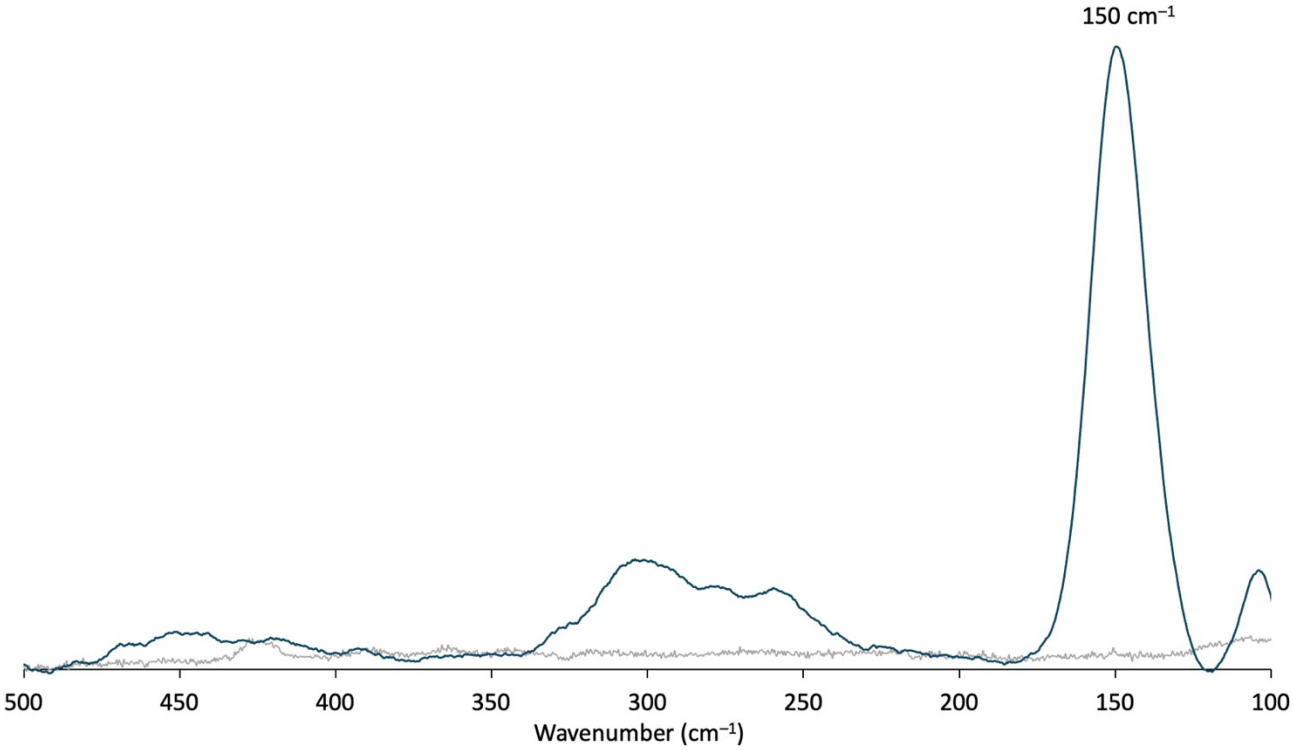

Figure S3. Raman spectra of **BTR** (gray) and **BTR•I_2** (blue) focused on I-I stretching region (100–500 cm^{-1}).

5. Computational details

The computational investigation on **BTR** and **BTR•I_2** was carried out at the DFT level by the Gaussian 16 suite of programs.[6] A preliminary validation of the computational setup was carried out by comparing selected optimized distances for **BTR** with the corresponding structural data. The mPW1PW functional[7] was adopted in combination with LANL08(d)[8] basis sets (BSs) with Relativistic Effective Core Potentials (RECPs) on the heavier iodine species, and by adopting Def2-SVP[9] BSs on the lighter elements (C, H, N, O, and S). Basis sets were obtained from Basis Set Exchange and Basis Set EMSL Library. The memory required for each calculation was evaluated by the GaussMem cross-platform (Linux, macOS, Windows) program as a function of the number of shared processors, the total number of basis set functions, and a memory threshold depending on the highest angular momentum basis function.[10] The molecular geometry optimizations (Tables S6–S11) were performed starting from the available structural data. The nature of the minima of each optimized geometry was verified by harmonic frequency calculations. In the case of **BTR**, two different geometries were optimized, corresponding to the periplanar and antiperiplanar conformation of the bithiophene moiety. Charge distributions and Wiberg bond indices[11] were evaluated at the NBO level at the optimized geometries. The program GaussView 6.1.1[12] was used to investigate the optimized structures, the isosurfaces of Kohn–Sham molecular orbitals, and the MEP maps.

4.1. Computational Analysis

Table S6. Optimized geometry calculated for compound **BTR** at DFT level [mPW1PW//def2-SVP/LANL08(d)] in the gas phase in orthogonal Cartesian coordinate format (periplanar conformer).

Center Number	Atomic Number	Atomic Type	Coordinates (Angstroms) X	Y	Z
1	16	0	2.231022	6.973133	5.825206
2	16	0	3.952281	9.399969	5.630503
3	16	0	0.637490	4.244181	5.151760
4	16	0	0.893183	2.232430	2.544005
5	8	0	1.331941	7.647986	9.489364
6	7	0	2.591033	8.585239	7.808853
7	6	0	2.965571	8.429262	6.502965
8	6	0	1.423349	6.595333	7.330976
9	6	0	1.734828	7.619398	8.350494
10	6	0	3.030283	9.709028	8.626250
11	1	0	4.059166	9.941342	8.320635
12	1	0	3.033337	9.345292	9.661839
13	6	0	0.613568	5.548801	7.630289
14	1	0	0.238133	5.554225	8.658489
15	6	0	-0.263365	2.771605	5.017522
16	6	0	2.133889	10.926569	8.483017
17	1	0	2.125135	11.286284	7.445311
18	1	0	2.507768	11.738785	9.121827
19	1	0	1.104998	10.697392	8.792341
20	6	0	0.183800	4.457092	6.817784
21	6	0	-0.307574	2.023798	3.780289
22	6	0	0.145127	1.068413	1.531631
23	1	0	0.573500	0.840303	0.557985
24	6	0	-0.972926	0.529917	2.114553
25	1	0	-1.592683	-0.226898	1.635191
26	6	0	-0.647319	3.420178	7.221417
27	1	0	-1.047987	3.358633	8.232991
28	6	0	-0.896144	2.473490	6.214438
29	1	0	-1.501763	1.579499	6.353885
30	6	0	-1.234747	1.074208	3.396066
31	1	0	-2.089361	0.797919	4.012158

Table S7. Optimized geometry calculated for compound **BTR** at DFT level [mPW1PW//def2-SVP/LANL08(d)] in the gas phase in orthogonal Cartesian coordinate format (antiperiplanar conformer).

Center Number	Atomic Number	Coordinates (Angstroms) X	Y	Z
1	16	2.544743	5.652302	1.103449
2	16	2.951428	8.488095	1.929296
3	16	3.009963	2.530037	0.426965
4	16	4.295246	-1.598879	-0.311517
5	8	-1.183354	6.175199	0.385523
6	7	0.631982	7.385036	1.112933
7	6	1.967298	7.295936	1.392825
8	6	0.958124	5.107306	0.605136
9	6	-0.009190	6.223140	0.666850
10	6	-0.119901	8.626668	1.243528
11	1	0.293908	9.159208	2.110214
12	1	-1.154478	8.330921	1.460190
13	6	0.562421	3.872683	0.204795
14	1	-0.499071	3.805687	-0.053880
15	6	3.038139	0.849342	0.009377
16	6	-0.053731	9.488669	-0.005070
17	1	0.982273	9.778826	-0.226019
18	1	-0.639229	10.406069	0.146982
19	1	-0.471157	8.959235	-0.872406
20	6	1.311516	2.665656	0.072550
21	6	4.263119	0.089128	0.097327
22	6	5.970654	-1.716066	0.035683
23	1	6.483964	-2.667819	-0.083743
24	6	6.491152	-0.517160	0.448530
25	1	7.537346	-0.378363	0.717913
26	6	0.812698	1.440640	-0.349877
27	1	-0.232988	1.302641	-0.623505
28	6	1.779484	0.422853	-0.385722
29	1	1.573353	-0.602545	-0.691626
30	6	5.519698	0.513350	0.484242
31	1	5.732249	1.539526	0.784586

Table S8. Optimized geometry calculated for compound **BTR•I_2** at DFT level [mPW1PW//def2-SVP/LANL08(d)] in the gas phase in orthogonal Cartesian coordinate format.

Center Number	Atomic Number	Coordinates (Angstroms) X	Y	Z
1	53	4.252388	8.044883	3.083485
2	53	4.449911	6.783650	0.614151
3	16	2.248162	6.936160	5.869865
4	16	4.020507	9.359673	5.715268
5	16	0.643274	4.249703	5.170463
6	16	0.885422	2.310456	2.531065
7	8	1.288938	7.676148	9.512090
8	7	2.596167	8.565132	7.837842
9	6	2.979674	8.371574	6.552016
10	6	1.402712	6.594279	7.368067
11	6	1.705412	7.615394	8.381308
12	6	3.038200	9.692848	8.652506
13	1	4.086654	9.889932	8.390567
14	1	2.991333	9.342568	9.691530
15	6	0.570352	5.555482	7.644862
16	1	0.167216	5.567028	8.662707
17	6	-0.268366	2.787904	5.017386
18	6	2.179932	10.930985	8.460804
19	1	2.209402	11.278259	7.419282
20	1	2.556849	11.741401	9.099629
21	1	1.136925	10.733664	8.742911
22	6	0.150866	4.470786	6.824927
23	6	-0.286725	2.039073	3.782268
24	6	0.183972	1.111949	1.529332
25	1	0.612501	0.906552	0.550609
26	6	-0.899832	0.516496	2.123913
27	1	-1.485891	-0.270063	1.650377
28	6	-0.701468	3.441231	7.210612
29	1	-1.128030	3.385418	8.211975
30	6	-0.934928	2.497456	6.201117
31	1	-1.555340	1.611827	6.326416
32	6	-1.171500	1.043937	3.408737
33	1	-2.001547	0.720916	4.035568

Table S9. Natural population analysis for compound **BTR** at the DFT-optimized geometry [mPW1PW//def2-SVP/LANL08(d)] in the gas phase (periplanar conformation).

Atom	No	Natural Charge	Core	Valence	Rydberg	Total
S	1	0.37430	9.99880	5.58953	0.03736	15.62570
S	2	-0.06373	9.99898	6.03426	0.03049	16.06373
S	3	0.43049	9.99875	5.53564	0.03511	15.56951
S	4	0.43011	9.99880	5.53357	0.03751	15.56989
O	5	-0.59126	1.99972	6.58148	0.01006	8.59126
N	6	-0.50180	1.99891	5.48861	0.01428	7.50180
C	7	-0.08982	1.99929	4.04850	0.04202	6.08982
C	8	-0.30131	1.99887	4.28054	0.02190	6.30131
C	9	0.71454	1.99911	3.23654	0.04982	5.28546
C	10	-0.22573	1.99918	4.20651	0.02004	6.22573
H	11	0.24301	0.00000	0.75203	0.00495	0.75699
H	12	0.24526	0.00000	0.75027	0.00447	0.75474
C	13	-0.18033	1.99885	4.15717	0.02431	6.18033
H	14	0.26710	0.00000	0.72828	0.00462	0.73290
C	15	-0.19710	1.99891	4.17306	0.02512	6.19710
C	16	-0.65046	1.99925	4.64377	0.00745	6.65046
H	17	0.22925	0.00000	0.76744	0.00331	0.77075
H	18	0.23016	0.00000	0.76771	0.00213	0.76984
H	19	0.22534	0.00000	0.77201	0.00265	0.77466
C	20	-0.23455	1.99892	4.21464	0.02100	6.23455
C	21	-0.23794	1.99890	4.21399	0.02506	6.23794
C	22	-0.39950	1.99903	4.38164	0.01884	6.39950
H	23	0.25646	0.00000	0.74172	0.00183	0.74354
C	24	-0.26476	1.99890	4.25003	0.01583	6.26476
H	25	0.24467	0.00000	0.75293	0.00239	0.75533
C	26	-0.20730	1.99885	4.19206	0.01639	6.20730
H	27	0.24677	0.00000	0.75091	0.00233	0.75323
C	28	-0.24554	1.99884	4.23052	0.01618	6.24554
H	29	0.24609	0.00000	0.75152	0.00240	0.75391
C	30	-0.23449	1.99885	4.21967	0.01598	6.23449
H	31	0.24208	0.00000	0.75551	0.00241	0.75792

Table S10. Natural population analysis for compound **BTR** at the DFT-optimized geometry [mPW1PW//def2-SVP/LANL08(d)] in the gas phase (antiperiplanar conformation).

Atom	No	Natural Charge	Core	Valence	Rydberg	Total
S	1	0.37268	9.99880	5.59117	0.03735	15.62732
S	2	-0.06479	9.99898	6.03533	0.03048	16.06479
S	3	0.42754	9.99876	5.53884	0.03486	15.57246
S	4	0.42348	9.99880	5.54044	0.03727	15.57652
O	5	-0.59105	1.99972	6.58126	0.01006	8.59105
N	6	-0.50171	1.99891	5.48851	0.01428	7.50171
C	7	-0.08951	1.99929	4.04821	0.04200	6.08951
C	8	-0.30142	1.99887	4.28067	0.02189	6.30142
C	9	0.71432	1.99911	3.23677	0.04981	5.28568
C	10	-0.22573	1.99918	4.20652	0.02004	6.22573
H	11	0.24299	0.00000	0.75206	0.00495	0.75701
H	12	0.24536	0.00000	0.75016	0.00447	0.75464
C	13	-0.18026	1.99885	4.15713	0.02428	6.18026
H	14	0.26731	0.00000	0.72808	0.00461	0.73269
C	15	-0.19489	1.99890	4.17124	0.02474	6.19489
C	16	-0.65048	1.99925	4.64378	0.00745	6.65048
H	17	0.22921	0.00000	0.76749	0.00331	0.77079
H	18	0.23023	0.00000	0.76764	0.00213	0.76977
H	19	0.22539	0.00000	0.77196	0.00265	0.77461
C	20	-0.23268	1.99891	4.21286	0.02091	6.23268
C	21	-0.23514	1.99889	4.21154	0.02471	6.23514
C	22	-0.39722	1.99903	4.37956	0.01863	6.39722
H	23	0.25617	0.00000	0.74200	0.00184	0.74383
C	24	-0.26327	1.99890	4.24831	0.01605	6.26327
H	25	0.24571	0.00000	0.75192	0.00237	0.75429
C	26	-0.20623	1.99886	4.19076	0.01661	6.20623
H	27	0.24719	0.00000	0.75049	0.00232	0.75281
C	28	-0.25034	1.99885	4.23580	0.01568	6.25034
H	29	0.24816	0.00000	0.74931	0.00253	0.75184
C	30	-0.23715	1.99885	4.22275	0.01555	6.23715
H	31	0.24612	0.00000	0.75138	0.00251	0.75388

Table S11. Natural population analysis for compound **BTR•I_2** at the DFT-optimized geometry [mPW1PW//def2-SVP/LANL08(d)] in the gas phase.

Atom	No	Natural Charge	Core	Valence	Rydberg	Total
I	1	-0.02827	46.00000	7.00783	0.02044	53.02827
I	2	-0.18357	46.00000	7.16704	0.01653	53.18357
S	3	0.41732	9.99877	5.54593	0.03798	15.58268
S	4	-0.01991	9.99895	5.98685	0.03411	16.01991
S	5	0.43943	9.99875	5.52671	0.03512	15.56057
S	6	0.44506	9.99880	5.51843	0.03771	15.55494
O	7	-0.58101	1.99972	6.57116	0.01013	8.58101
N	8	-0.49155	1.99891	5.47842	0.01422	7.49155
C	9	-0.05883	1.99926	4.02185	0.03772	6.05883
C	10	-0.31447	1.99886	4.29356	0.02204	6.31447
C	11	0.71211	1.99910	3.23881	0.04999	5.28789
C	12	-0.22863	1.99918	4.20974	0.01972	6.22863
H	13	0.24304	0.00000	0.75279	0.00417	0.75696
H	14	0.25118	0.00000	0.74432	0.00450	0.74882
C	15	-0.15853	1.99885	4.13544	0.02424	6.15853
H	16	0.26894	0.00000	0.72655	0.00452	0.73106
C	17	-0.18308	1.99892	4.15898	0.02518	6.18308
C	18	-0.65200	1.99925	4.64516	0.00760	6.65200
H	19	0.23036	0.00000	0.76666	0.00298	0.76964
H	20	0.23469	0.00000	0.76321	0.00210	0.76531
H	21	0.22827	0.00000	0.76913	0.00260	0.77173
C	22	-0.24429	1.99892	4.22447	0.02091	6.24429
C	23	-0.24484	1.99890	4.22077	0.02518	6.24484
C	24	-0.39133	1.99903	4.37337	0.01893	6.39133
H	25	0.25949	0.00000	0.73869	0.00182	0.74051
C	26	-0.26543	1.99890	4.25068	0.01584	6.26543
H	27	0.24638	0.00000	0.75124	0.00238	0.75362
C	28	-0.19445	1.99886	4.17915	0.01644	6.19445
H	29	0.24835	0.00000	0.74933	0.00232	0.75165
C	30	-0.24790	1.99885	4.23286	0.01619	6.24790
H	31	0.24805	0.00000	0.74957	0.00238	0.75195
C	32	-0.22658	1.99885	4.21176	0.01596	6.22658
H	33	0.24200	0.00000	0.75558	0.00241	0.75800

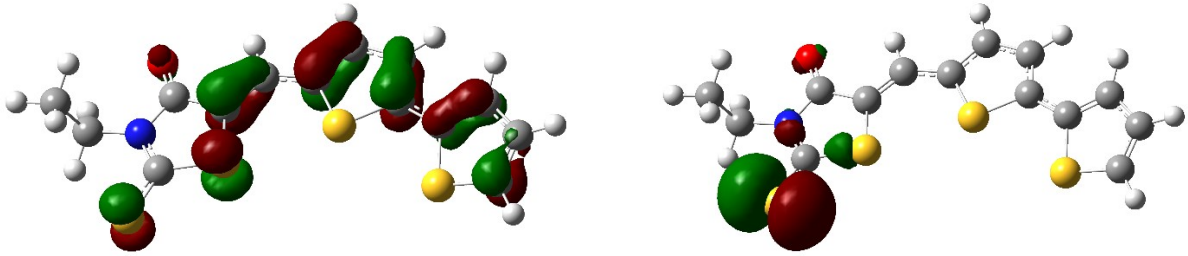

(a) (b)

Figure S4. Isosurfaces of KS-HOMO (a) and KS-HOMO-1 calculated for **BTR** at DFT level (periplanar conformer). Color: carbon, gray; nitrogen, blue; oxygen, red; sulfur, yellow; hydrogen, white. Cutoff value 0.05 |e|.

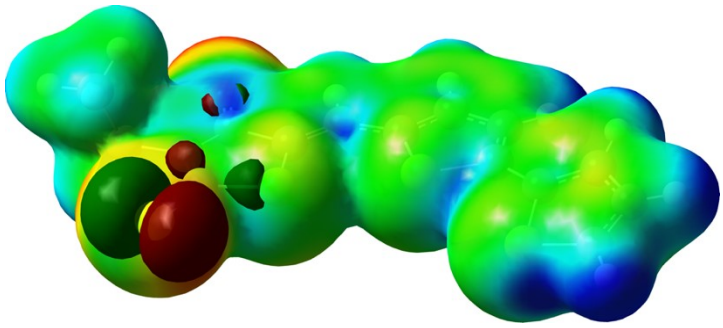

Figure S5. Superimposed molecular electrostatic potential mapped on the electron density ($5 \cdot 10^{-3}$ |e|·Bohr^{-3}) for the periplanar conformer of compound BTR [a; range –0.05 (red) to +0.06 (blue) a.u.] and KS-HOMO-1 isosurface (cutoff value = 0.05 |e|).

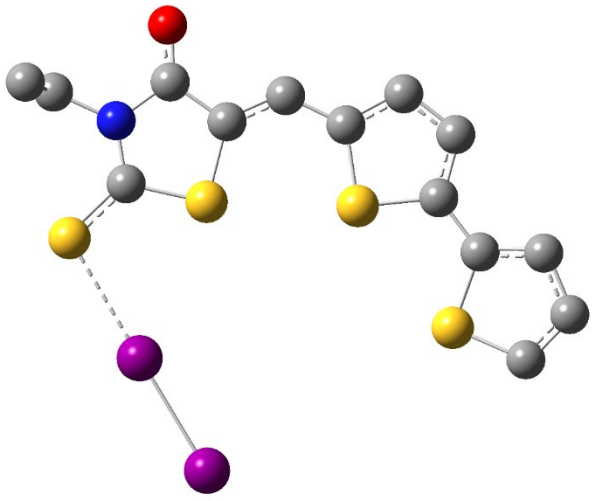

Figure S6. Ball and stick representation of the 1:1 "spoke" adduct BTR·I_2 optimized at DFT level in the periplanar conformation. Color: carbon, gray; nitrogen, blue; oxygen, red; sulfur, yellow; hydrogen, white. Hydrogen atoms were omitted for clarity.

6. References

1. J. Yu, T. -L. Shen, W. -H. Weng, Y. -C. Huang, C. Huang, W. -F. Su, S. -P. Rwei, K. -C. Ho, L. Wang, Molecular Design of Interfacial Modifiers for Polymer-Inorganic Hybrid Solar Cells, *Adv. Energy Mater.,* 2012, **2**, 245–252.
2. T. Khanasa, N. Jantasing, S. Morada, N. Leesakul, R. Tarsang, S. Namuangruk, T. Kaewin, S. Jungsuttiwong, T. Sudyoadsuk, V. Promarak, Synthesis and Characterization of 2D-D-π-A-Type Organic Dyes Bearing Bis(3,6-di-tert-butylcarbazol-9-ylphenyl)aniline as Donor Moiety for Dye-Sensitized Solar Cells, *Eur. J. Org. Chem*., 2013, 2608–2620.
3. G. M. Sheldrick, SHELXT - Integrated Space-Group and Crystal-Structure Determination, *Acta Cryst. A*, 2015, **71** , 3–8.
4. G. M. Sheldrick, Crystal Structure Refinement with SHELXL, *Acta Cryst. C*, 2015, **71**, 3–8.
5. O. V. Dolomanov,L. J. Bourhis, R. J. Gildea, J. A. K. Howard,H. Puschmann, OLEX2: A Complete Structure Solution, Refinement and Analysis Program, *J. Appl. Cryst.*, 2009, **42**, 339–341.
6. Gaussian 16, Revision C.01, M. J. Frisch, G. W. Trucks, H. B. Schlegel, G. E. Scuseria, M. A. Robb, J. R. Cheeseman, G. Scalmani, V. Barone, G. A. Petersson, H. Nakatsuji, X. Li, M. Caricato, A. V. Marenich, J. Bloino, B. G. Janesko, R. Gomperts, B. Mennucci, H. P. Hratchian, J. V. Ortiz, A. F. Izmaylov, J. L. Sonnenberg, D. Williams-Young, F. Ding, F. Lipparini, F. Egidi, J. Goings, B. Peng, A. Petrone, T. Henderson, D. Ranasinghe, V. G. Zakrzewski, J. Gao, N. Rega, G. Zheng, W. Liang, M. Hada, M. Ehara, K. Toyota, R. Fukuda, J. Hasegawa, M. Ishida, T. Nakajima, Y. Honda, O. Kitao, H. Nakai, T. Vreven, K. Throssell, J. A. Montgomery, Jr., J. E. Peralta, F. Ogliaro, M. J. Bearpark, J. J. Heyd, E. N. Brothers, K. N. Kudin, V. N. Staroverov, T. A. Keith, R. Kobayashi, J. Normand, K. Raghavachari, A. P. Rendell, J. C. Burant, S. S. Iyengar, J. Tomasi, M. Cossi, J. M. Millam, M. Klene, C. Adamo, R. Cammi, J. W. Ochterski, R. L. Martin, K. Morokuma, O. Farkas, J. B. Foresman, D. J. Fox, Gaussian, Inc., Wallingford CT, 2016.
7. C. Adamo, V. Barone, Exchange functionals with improved long-range behavior and adiabatic connection methods without adjustable parameters: The mPW and mPW1PW models, *J. Chem. Phys.*, 1998, **108**, 664–675.
8. L. E. Roy, P. J. Hay, R. L. Martin, Revised Basis Sets for the LANL Effective Core Potentials, *J. Chem. Theory Comput*., 2008, **4**, 1029–1031.
9 F. Weigend, R. Ahlrichs, Balanced basis sets of split valence, triple zeta valence and quadruple zeta valence quality for H to Rn: Design and assessment of accuracy, *Phys. Chem. Chem. Phys*., 2005, **7**, 3297–3305.
10. GaussMem, rev. 2024, M. Arca, https://massimiliano-arca.itch.io/gaussmem
11. K. B. Wiberg, Application of the pople-santry-segal CNDO method to the cyclopropylcarbinyl and cyclobutyl cation and to cyclobutane, *Tetrahedron* 1968, **24**, 1083–1096.
12. GaussView, Version 6.1.1, R. Dennington, T. A. Keith, J. M. Millam, Semichem Inc., Shawnee Mission, KS, 2016.